

Absence of Magnetic Thermal Conductivity in the Quantum Spin Liquid Candidate $\text{EtMe}_3\text{Sb}[\text{Pd}(\text{dmit})_2]_2$

J. M. Ni,¹ B. L. Pan,¹ B. Q. Song,¹ Y. Y. Huang,¹ J. Y. Zeng,¹ Y. J. Yu,¹ E. J. Cheng,¹ L. S. Wang,¹
D. Z. Dai,¹ R. Kato² and S. Y. Li^{1,3,*}

¹State Key Laboratory of Surface Physics, Department of Physics, and Laboratory of Advanced Materials, Fudan University, Shanghai 200438, China

²RIKEN, Condensed Molecular Materials Laboratory, Wako 351-0198, Japan

³Collaborative Innovation Center of Advanced Microstructures, Nanjing 210093, China

 (Received 30 April 2019; revised manuscript received 7 June 2019; published 10 December 2019)

We present the ultralow-temperature specific heat and thermal conductivity measurements on single crystals of triangular-lattice compound $\text{EtMe}_3\text{Sb}[\text{Pd}(\text{dmit})_2]_2$, which has long been considered as a gapless quantum spin liquid candidate. In specific heat measurements, a finite linear term is observed, consistent with the previous work [S. Yamashita *et al.*, *Nat. Commun.* **2**, 275 (2011)]. However, we do not observe a finite residual linear term in the thermal conductivity measurements, and the thermal conductivity does not change in a magnetic field of 6 T. These results are in sharp contrast to previous thermal conductivity measurements on $\text{EtMe}_3\text{Sb}[\text{Pd}(\text{dmit})_2]_2$ [M. Yamashita *et al.*, *Science* **328**, 1246 (2010)], in which a huge residual linear term was observed and attributed to highly mobile gapless excitations, likely the spinons of a quantum spin liquid. In this context, the true ground state of $\text{EtMe}_3\text{Sb}[\text{Pd}(\text{dmit})_2]_2$ has to be reconsidered.

DOI: 10.1103/PhysRevLett.123.247204

Quantum spin liquid (QSL) states have been one of the central issues in condensed matter physics since the seminal proposal by Anderson [1,2]. Because of the strong geometrical frustration and quantum fluctuations, the spins do not order even down to zero temperature and remain highly entangled, and fractionalized excitations called spinons are the most pronounced characteristic in QSL states [3–5]. The detection and study of these excitations are of great importance to give information about the nature of QSL states. As the prototype of a QSL in Anderson's resonating valence bond model [1], the spin 1/2 triangular-lattice Heisenberg antiferromagnet is a platform for searching the QSL candidates. Among those triangular-lattice QSL candidates, the two organic compounds $\kappa\text{-(BEDT-TTF)}_2\text{Cu}_2(\text{CN})_3$ and $\text{EtMe}_3\text{Sb}[\text{Pd}(\text{dmit})_2]_2$ seem to be promising [6–16], while the inorganic compound YbMgGaO_4 is under hot debate [17–23].

$\text{EtMe}_3\text{Sb}[\text{Pd}(\text{dmit})_2]_2$ (Me = CH₃, Et = C₂H₅, dmit = 1,3-dithiole-2-thione-4,5-dithiolate) is a compound of the series of layered organic salts $\beta\text{'-}X[\text{Pd}(\text{dmit})_2]_2$, where X is a nonmagnetic cation, and $\text{Pd}(\text{dmit})_2$ is highly dimerized forming the spin 1/2 anion $[\text{Pd}(\text{dmit})_2]_2^-$ [24,25]. Each $\text{Pd}(\text{dmit})_2$ layer is parallel to the ab plane and is separated by the EtMe_3Sb^+ cation layer, as seen in Fig. 1(a) (cation layers are not shown for clarity). The dimerized $\text{Pd}(\text{dmit})_2$ are arranged to form a triangular lattice in the layer, causing a strong geometrical frustration of spins on the dimers, illustrated in Fig. 1(b). No signature of long range magnetic order was observed down to about 20 mK by nuclear magnetic resonance (NMR) measurements [13,14], in spite

of the large effective antiferromagnetic exchange interactions of the order of 250 K [11]. However, the deviation of NMR spin-lattice relaxation curves from single exponential functions below 10 K indicates that the spin state gradually becomes inhomogeneous [13,14]. As for the study of excitations in this putative QSL candidate, the spin-lattice relaxation $1/T_1$ was found to follow the T^2 temperature dependence below 1 K, indicating a nodal spin gap [13,14]. In contrast, a finite linear term γ of 19.9 mJ K⁻² mol⁻¹ was observed in the specific heat measurements, implying the existence of gapless fermionic excitations [15]. The gapless nature was further confirmed by the torque magnetometry, which revealed residual paramagnetic susceptibility comparable to that in metal [16].

More strikingly, the previous thermal conductivity work of $\text{EtMe}_3\text{Sb}[\text{Pd}(\text{dmit})_2]_2$ single crystals by M. Yamashita *et al.* [12] reported the observation of a huge residual linear term κ_0/T of 2 mW K⁻² cm⁻¹, which is attributed to highly mobile gapless fermionic excitations with the mean free path as long as 1000 interspin distances. This is a strong evidence for the existence of a spinon Fermi surface in such a QSL candidate, stimulating a number of theoretical studies [4,5]. The enhancement of κ above 2 T was also observed [12]. However, for the other two triangular-lattice QSL candidates $\kappa\text{-(BEDT-TTF)}_2\text{Cu}_2(\text{CN})_3$ and YbMgGaO_4 , no residual linear terms were found in thermal conductivity measurements [9,20], although they also display a gapless nature in specific heat measurements [i.e., a linear term γ of 15 mJ K⁻² mol⁻¹ in $\kappa\text{-(BEDT-TTF)}_2\text{Cu}_2(\text{CN})_3$ and a power-law temperature dependence in YbMgGaO_4 ,

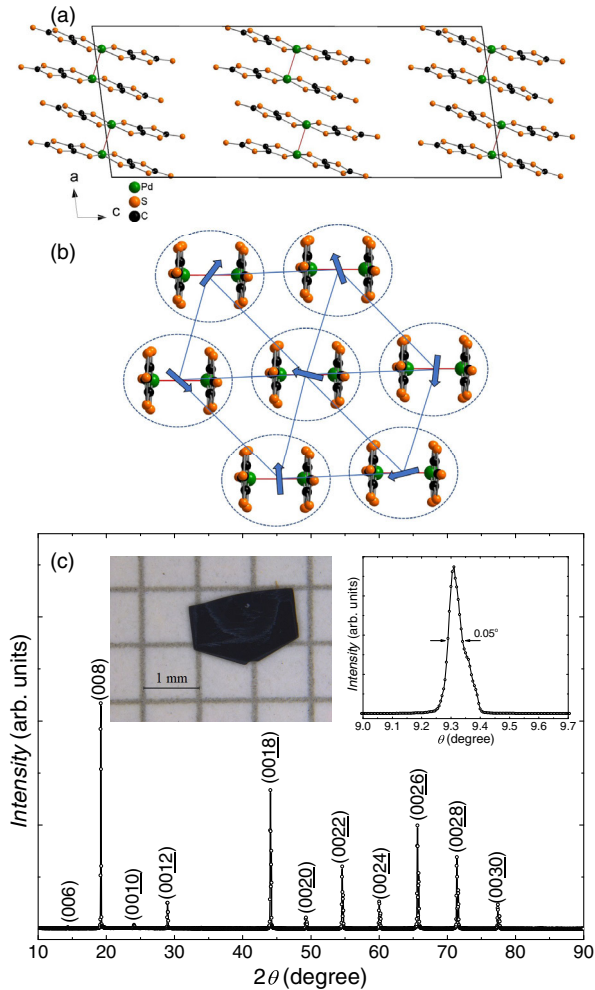


FIG. 1. (a) Crystal structure of $\text{EtMe}_3\text{Sb}[\text{Pd}(\text{dmit})_2]_2$ with only the $\text{Pd}(\text{dmit})_2$ layers shown. (b) The triangular-lattice structure of the spin $1/2$ in the $\text{Pd}(\text{dmit})_2$ layer. The dimerized $\text{Pd}(\text{dmit})_2$ are surrounded by dashed ovals. Each $1/2$ spin, denoted as a blue arrow, is localized on each dimer. (c) Room-temperature XRD pattern from the natural surface of the $\text{EtMe}_3\text{Sb}[\text{Pd}(\text{dmit})_2]_2$ single crystal. Left inset: the photo of a typical $\text{EtMe}_3\text{Sb}[\text{Pd}(\text{dmit})_2]_2$ single crystal. Right inset: x-ray rocking scan curve of the (008) Bragg peak.

respectively] [8,17,20]. One may raise the question why $\text{EtMe}_3\text{Sb}[\text{Pd}(\text{dmit})_2]_2$ is so different from other triangular-lattice QSL candidates. Therefore, as the vital experimental foundation of many theoretical works, it is desired to revisit these thermodynamic and transport properties of $\text{EtMe}_3\text{Sb}[\text{Pd}(\text{dmit})_2]_2$.

In this Letter, we report the ultralow-temperature specific heat and thermal conductivity measurements on high-quality $\text{EtMe}_3\text{Sb}[\text{Pd}(\text{dmit})_2]_2$ single crystals. A linear term γ of $15 \text{ mJ K}^{-2} \text{ cm}^{-1}$ is found in the specific heat, which is consistent with the previous work [15]. However, it is unsuccessful to reproduce previous thermal conductivity results reported in Ref. [12]. A negligible residual linear term κ_0/T is observed, implying the absence of mobile

gapless fermionic excitations. This raises the question about the true ground state of this triangular-lattice QSL candidate.

Single crystals of $\text{EtMe}_3\text{Sb}[\text{Pd}(\text{dmit})_2]_2$ were provided by the same group at RIKEN as in Ref. [12]. The photo and the typical x-ray diffraction (XRD) pattern (measured by a D8 Advance x-ray diffractometer from Bruker) from the natural ab plane of a $\text{EtMe}_3\text{Sb}[\text{Pd}(\text{dmit})_2]_2$ sample are shown in Fig. 1(c). The full width at half-maximum (FWHM) of the x-ray rocking scan curve of the (008) Bragg peak is only 0.05° , indicating the high quality of the samples. The specific heat of a sample with $0.4 \pm 0.1 \text{ mg}$ was measured by the relaxation method in a physical property measurement system (Quantum Design) equipped with a ^3He cryostat. Since stacking more samples together will lead to a bad thermal contact, we only measured the specific heat of one large sample with comparable size of the sample holder. The light mass of the sample is due to its low density and small thickness. Samples for thermal conductivity measurements have the dimensions of $1.34 \times 0.60 \times 0.05 \text{ mm}^3$ for sample 1, $2.00 \times 1.17 \times 0.05 \text{ mm}^3$ for sample 2, and $1.34 \times 0.88 \times 0.02 \text{ mm}^3$ for sample 3, respectively. Note that the samples used for thermal conductivity measurements come from three different batches. All samples were prepared in almost the same conditions as samples in Ref. [12]. As for sample 3, especially, the conditions were the same including the reagents. Contacts of sample 1 were made using gold paste. Contacts of samples 2 and 3 were made using carbon paste. The thermal conductivity was measured in a dilution refrigerator, using a standard four-wire steady-state method. Samples were cooled slowly from room temperature to the lowest temperature for two days in order to avoid cracks. Magnetic fields were applied perpendicular to the ab plane. A scanning electron microscope (SEM, Zeiss EVO-10) was used to examine the surface of sample 1 after thermal conductivity measurements.

The temperature dependence of the specific heat of $\text{EtMe}_3\text{Sb}[\text{Pd}(\text{dmit})_2]_2$ single crystal from 0.65 to 4 K at zero field is shown in the inset of Fig. 2. The main panel of Fig. 2 plots the C/T vs T^2 below 2 K. The upturn at low temperatures is attributed to the Schottky anomaly [15]. C/T can be well fitted by the formula $C/T = \gamma + \beta T^2$ between 0.9 and 2 K, giving $\gamma = 15 \pm 4 \text{ mJ K}^{-2} \text{ mol}^{-1}$ and $\beta = 17 \pm 4 \text{ mJ K}^{-4} \text{ mol}^{-1}$ after considering the error in mass. This behavior is similar to that in Ref. [15], which is also plotted in Fig. 2. Actually, if we scale our data by a factor of 1.36, they are on top of the curve in Ref. [15]. Thus, the previous specific heat result is well reproduced by us, and the slight difference is likely due to the uncertainty in determining the mass of samples.

Since a specific heat result may be contaminated by nuclear contributions [8,15], the thermal transport measurement, a tool insensitive to localized excitations, would be more advantageous for identifying the

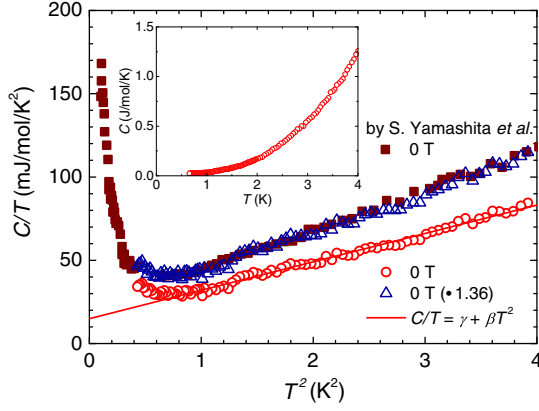


FIG. 2. Temperature dependence of the specific heat of $\text{EtMe}_3\text{Sb}[\text{Pd}(\text{dmit})_2]_2$ single crystal at zero field. The inset shows C vs T from 0.65 to 4 K. The main panel plots C/T vs T^2 below 2 K. The solid line is the fit to the specific heat data between 0.9 K and 2 K to $C/T = \gamma + \beta T^2$. A linear term $\gamma = 15 \pm 4 \text{ mJ K}^{-2} \text{ mol}^{-1}$ is obtained. For comparison, the specific heat result in Ref. [15] is also plotted. Scaling by a factor of 1.36 can well reproduce the prior result, indicating that the difference is likely due to the uncertainty in measuring the mass of the samples.

low-energy excitations in a QSL candidate. Figure 3(a) presents the in-plane zero-field thermal conductivity of $\text{EtMe}_3\text{Sb}[\text{Pd}(\text{dmit})_2]_2$ single crystals with two kinds of contacts, respectively. The thermal conductivity of an insulating QSL candidate at very low temperatures usually can be fitted by $\kappa/T = a + bT^{\alpha-1}$, in which the two terms aT and bT^{α} represent the contributions from itinerant gapless fermionic magnetic excitations (if they do exist) and phonons, respectively. For phonons, the power α is typically between two and three, due to the specular reflections at the sample surfaces [26,27]. As can be seen in Fig. 3(a), similar thermal conductivity results between samples with gold and carbon pasted contacts are observed. Furthermore, contrary to Ref. [12], where κ/T shows T^2 temperature dependence, a linear fitting $\kappa/T = a + bT$ is more suitable for our samples 1 and 2. The fitting gives the value of κ_0/T of $0.004 \pm 0.009 \text{ mW K}^{-2} \text{ cm}^{-1}$ and $0.004 \pm 0.005 \text{ mW K}^{-2} \text{ cm}^{-1}$ for samples 1 and 2, respectively. Considering the experimental error bar of $5 \mu\text{W K}^{-2} \text{ cm}^{-1}$, the κ_0/T of both samples at $\mu_0 H = 0 \text{ T}$ are virtually zero. The behavior of sample 3 is very similar to samples 1 and 2. Because of the slightly sub-linear temperature dependence, it extrapolates to a small negative value of κ_0/T . Therefore, previous huge κ_0/T of $\text{EtMe}_3\text{Sb}[\text{Pd}(\text{dmit})_2]_2$ in Ref. [12] can not be reproduced in any of our samples.

The in-plane thermal conductivities of sample 2 at $\mu_0 H = 0$ and 6 T are plotted in Fig. 3(b). The magnetic field barely has any effect on the thermal conductivity of $\text{EtMe}_3\text{Sb}[\text{Pd}(\text{dmit})_2]_2$ at 6 T. This magnetic field dependence, again, is in stark contrast to the previous measurements

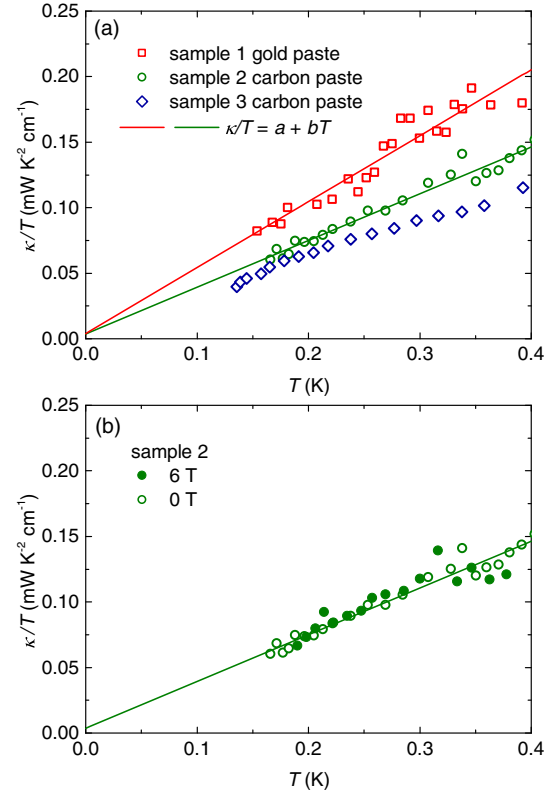


FIG. 3. (a) The zero-field in-plane thermal conductivity of three $\text{EtMe}_3\text{Sb}[\text{Pd}(\text{dmit})_2]_2$ single crystals, using contacts of gold paste and carbon paste, respectively. (b) The in-plane thermal conductivity of sample 2 at $\mu_0 H = 0$ and 6 T. The straight lines are the fits to the zero-field thermal conductivity data to $\kappa/T = a + bT$.

that report a gradual increase of thermal conductivity above approximately 2 T below 1 K [12]. For example, the observed magnetothermal conductivity $[\kappa(H) - \kappa(0T)]/\kappa(0T)$ is larger than 20% at 6 T at 0.23 K, which was suggested as a consequence of additional excitations with a spin gap closing at 2 T [12]. Because of the coexistence of gapless and gapped excitations, a type II spin liquid was proposed for $\text{EtMe}_3\text{Sb}[\text{Pd}(\text{dmit})_2]_2$ [28]. Considering the negligible field effect presented here, one may reexamine the existence of this gapped excitation and the proposal of type II spin liquid.

Figure 4 displays the comparison of our thermal conductivity data with the data of $\text{EtMe}_3\text{Sb}[\text{Pd}(\text{dmit})_2]_2$ and $\text{Et}_2\text{Me}_2\text{Sb}[\text{Pd}(\text{dmit})_2]_2$ in Ref. [12] and κ -(BEDT-TTF) $_2\text{Cu}_2(\text{CN})_3$ in Ref. [9]. The absolute value of our data are much smaller than that in Ref. [12], even 10 times smaller than the nonmagnetic reference compound $\text{Et}_2\text{Me}_2\text{Sb}[\text{Pd}(\text{dmit})_2]_2$ [12]. The lack of κ_0/T , a negligible field effect in $\mu_0 H = 6 \text{ T}$, and very small absolute value, all demonstrate that the thermal conductivity is entirely contributed by phonons in our samples, and the phonons are strongly scattered. This is supported by the estimation of the mean free path l_p of phonons by the kinetic formula

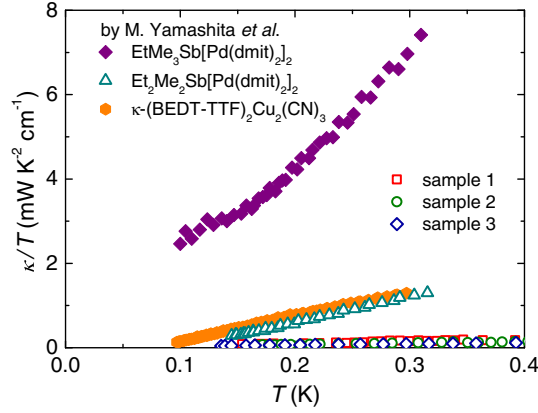


FIG. 4. Comparison of our thermal conductivity data with the data of $\text{EtMe}_3\text{Sb}[\text{Pd}(\text{dmit})_2]_2$ and $\text{Et}_2\text{Me}_2\text{Sb}[\text{Pd}(\text{dmit})_2]_2$ in Ref. [12] and $\kappa\text{-(BEDT-TTF)}_2\text{Cu}_2(\text{CN})_3$ in Ref. [9]. The absolute value of our data are much smaller than that in Ref. [12], even 10 times smaller than the nonmagnetic reference compound $\text{Et}_2\text{Me}_2\text{Sb}[\text{Pd}(\text{dmit})_2]_2$, indicating phonons being strongly scattered in our samples.

$\kappa = \frac{1}{3} C_p v_p l_p$, where $C_p = (2\pi^2 k_B/5)(k_B T/\hbar v_p)^3 = \beta T^3$ is the phonon specific heat and v_p is the velocity of phonons. With $\beta = 17 \text{ mJ K}^{-4} \text{ mol}^{-1}$ obtained by our specific heat measurement, v_p is estimated as $1.55 \times 10^3 \text{ m/s}$, giving l_p of sample 3 only about $5.88 \mu\text{m}$ at 0.3 K. Usually, when the sample enters the boundary scattering limit at sub-Kelvin temperatures, l_p should only be limited by the physical dimensions of the sample, resulting in a temperature independent $l_p = 2\sqrt{A/\pi}$, where A is the cross-sectional area of the sample [27]. For sample 3, the boundary limited l_p is $150 \mu\text{m}$. This is 25 times larger than l_p estimated from our thermal conductivity data and is consistent with the fact that the thermal conductivity of magnetic $\text{EtMe}_3\text{Sb}[\text{Pd}(\text{dmit})_2]_2$ is 10 times lower than the nonmagnetic $\text{Et}_2\text{Me}_2\text{Sb}[\text{Pd}(\text{dmit})_2]_2$. It is likely that the phonons are strongly scattered by those frustrated spins in $\text{EtMe}_3\text{Sb}[\text{Pd}(\text{dmit})_2]_2$. Note that, in another triangular-lattice system, the thermal conductivity of magnetic YbMgGaO_4 is about half of the nonmagnetic LuMgGaO_4 , again showing the scattering of phonons by the spins [20].

Now, we would like to discuss the implications of the negligible κ_0/T in $\text{EtMe}_3\text{Sb}[\text{Pd}(\text{dmit})_2]_2$ according to our new results. A gapless QSL may have fermionic spinons, which can form a Fermi surface like a metal, and provide a large density of states at low energies. Therefore, a sizable κ_0/T is expected [29–32]. In Ref. [12], from the observed huge $\kappa_0/T = 2 \text{ mW K}^{-2} \text{ cm}^{-1}$, the authors estimated the mean free path l_s of gapless fermionic excitations as long as 1000 interspin distances. However, according to the fitting result $\kappa_0/T = 0.004 \text{ mW K}^{-2} \text{ cm}^{-1}$ of our samples 1 and 2, an upper bound of l_s around 10 \AA is estimated, comparable to the interspin distance. In this context, the negligible κ_0/T observed in our experiments is inconsistent with the

existence of highly mobile gapless fermionic excitations and spinon Fermi surface in $\text{EtMe}_3\text{Sb}[\text{Pd}(\text{dmit})_2]_2$. The reason for such a huge discrepancy between our results and those in Ref. [12] is not clear for us, but it is clearly not due to intrinsic sample dependence since we have achieved similar results in three samples from different batches, especially including one prepared from the same conditions including the reagents as those in Ref. [12]. Also, it is not caused by the extrinsic factor of microcracks, since we do not detect microcracks on sample 1 with SEM after thermal conductivity measurements. Below, we only discuss the feasibility of possible scenarios in light of our experimental data on low-lying excitations.

One possible scenario is that $\text{EtMe}_3\text{Sb}[\text{Pd}(\text{dmit})_2]_2$ has a fully gapped ground state. This scenario was initially used to explain the absence of κ_0/T in $\kappa\text{-(BEDT-TTF)}_2\text{Cu}_2(\text{CN})_3$ [9]. By fitting the sublinear temperature-dependent κ/T at low temperature, a gap of about 0.46 K was obtained [9]. However, such a gapped scenario is inconsistent with the finite linear term in the specific heat. Therefore, the authors in Ref. [9] pointed out that the heat capacity measurements incorrectly suggest the presence of gapless excitation, possibly owing to the large Schottky contribution at low temperatures. Now that similar phenomena appear in $\text{EtMe}_3\text{Sb}[\text{Pd}(\text{dmit})_2]_2$, one may take both compounds into account for this scenario.

Another possible scenario is that gapless excitations do exist in $\text{EtMe}_3\text{Sb}[\text{Pd}(\text{dmit})_2]_2$ and $\kappa\text{-(BEDT-TTF)}_2\text{Cu}_2(\text{CN})_3$, indicated by specific heat measurements, but they are localized. Organic molecular compounds are generally thought of as extremely clean with a very low level of crystallographic defects. However, the exponent in the stretched-exponential fitting of the relaxation curve in NMR measurements of $\kappa\text{-(BEDT-TTF)}_2\text{Cu}_2(\text{CN})_3$ deviates from unity substantially below 6 K, indicating some inhomogeneity therein [7]. This scenario was considered as an alternative explanation for the negligible κ_0/T in $\kappa\text{-(BEDT-TTF)}_2\text{Cu}_2(\text{CN})_3$ [33]. For $\text{EtMe}_3\text{Sb}[\text{Pd}(\text{dmit})_2]_2$, the inhomogeneity was observed below 10 K in NMR measurements [13,14]. Although the stretching exponents which characterize the degree of inhomogeneity start to recover towards the homogeneous value below 1 K, they are only about 0.6 which still deviates from the value of a homogeneous system [13,14]. Thus, the inhomogeneity still cannot be ruled out in the sub-Kelvin temperature region [5]. Therefore, our thermal conductivity results raise the question regarding to what extent the inhomogeneity plays a role in the heat transport of $\text{EtMe}_3\text{Sb}[\text{Pd}(\text{dmit})_2]_2$.

Finally, a proposed random-singlet state, based on the quenched disorder on spin-1/2 quantum magnets, can induce the gapless QSL-like state [34–36]. The linear temperature dependence of specific heat may be an evidence for a power-law density of states of randomness [35,36]. Interestingly, the linear or sublinear temperature

dependence of our thermal conductivity κ/T is in agreement with the theoretical prediction for a random-singlet state [35]. This power law is a consequence of the scattering of acoustic phonons by quantum two-level systems from the distribution of random singlets [35], which may account for the huge suppression of our thermal conductivity shown in Fig. 4. However, we also notice that the specific heat is insensitive to the magnetic field and the susceptibility goes to a constant at low temperatures for $\text{EtMe}_3\text{Sb}[\text{Pd}(\text{dmit})_2]_2$ [11,15], which are not consistent with the random singlet model.

In summary, we have revisited the thermodynamic and heat transport properties of triangular-lattice organic QSL candidate $\text{EtMe}_3\text{Sb}[\text{Pd}(\text{dmit})_2]_2$. A linear term in the specific heat is well reproduced, as in the previous report [15], but the thermal conductivity shows a completely different behavior from Ref. [12]. No residual linear term κ_0/T is observed at the zero-temperature limit, suggesting the absence of mobile gapless fermionic excitations in $\text{EtMe}_3\text{Sb}[\text{Pd}(\text{dmit})_2]_2$. A magnetic field of 6 T does not affect the thermal conductivity, and its absolute value is even 10 times smaller than the nonmagnetic reference compound $\text{Et}_2\text{Me}_2\text{Sb}[\text{Pd}(\text{dmit})_2]_2$. We conclude that there is no magnetic thermal conductivity but only the phonon thermal conductivity in $\text{EtMe}_3\text{Sb}[\text{Pd}(\text{dmit})_2]_2$, and the phonons are strongly scattered by the frustrated spins. The absence of reproducible κ_0/T in any QSL candidates so far presents a direct challenge to the realization of a gapless QSL with highly mobile spinons in frustrated quantum magnets.

This work was supported by the Ministry of Science and Technology of China (Grants No. 2016YFA0300503 and No. 2015CB921401), the Natural Science Foundation of China (Grant No. 11421404), and the NSAF (Grant No. U1630248). It was also partially supported by the JSPS Grant-in-Aids for Scientific Research (S) (Grant No. JP16H06346).

Note added.—We are aware of a similar thermal conductivity study of $\text{EtMe}_3\text{Sb}[\text{Pd}(\text{dmit})_2]_2$ single crystals by the Taillefer group in Sherbrooke [37].

* shiyan_li@fudan.edu.cn

- [1] P. W. Anderson, Resonating valence bonds: A new kind of insulator?, *Mater. Res. Bull.* **8**, 153 (1973).
- [2] P. W. Anderson, The resonating valence bond state in La_2CuO_4 and superconductivity, *Science* **235**, 1196 (1987).
- [3] L. Balents, Spin liquids in frustrated magnets, *Nature (London)* **464**, 199 (2010).
- [4] L. Savary and L. Balents, Quantum spin liquids: A review, *Rep. Prog. Phys.* **80**, 016502 (2017).
- [5] Y. Zhou, K. Kanoda, and T. K. Ng, Quantum spin liquid states, *Rev. Mod. Phys.* **89**, 025003 (2017).
- [6] Y. Shimizu, K. Miyagawa, K. Kanoda, M. Maesato, and G. Saito, Spin-Liquid State in an Organic Mott Insulator with a Triangular Lattice, *Phys. Rev. Lett.* **91**, 107001 (2003).
- [7] Y. Shimizu, K. Miyagawa, K. Kanoda, M. Maesato, and G. Saito, Emergence of inhomogeneous moments from spin liquid in the triangular-lattice Mott insulator κ -(BEDT-TTF) $_2\text{Cu}_2(\text{CN})_3$, *Phys. Rev. B* **73**, 140407(R) (2006).
- [8] S. Yamashita, Y. Nakazawa, M. Oguni, Y. Oshima, H. Nojiri, Y. Shimizu, K. Miyagawa, and K. Kanoda, Thermodynamic properties of a spin-1/2 spin-liquid state in a κ -type organic salt, *Nat. Phys.* **4**, 459 (2008).
- [9] M. Yamashita, N. Nakata, Y. Kasahara, T. Sasaki, N. Yoneyama, N. Kobayashi, S. Fujimoto, T. Shibauchi, and Y. Matsuda, Thermal-transport measurements in a quantum spin-liquid state of the frustrated triangular magnet κ -(BEDT-TTF) $_2\text{Cu}_2(\text{CN})_3$, *Nat. Phys.* **5**, 44 (2009).
- [10] T. Itou, A. Oyamada, S. Maegawa, M. Tamura, and R. Kato, Spin-liquid state in an organic spin-1/2 system on a triangular lattice, $\text{EtMe}_3\text{Sb}[\text{Pd}(\text{dmit})_2]_2$, *J. Phys. Condens. Matter* **19**, 145247 (2007).
- [11] T. Itou, A. Oyamada, S. Maegawa, M. Tamura, and R. Kato, Quantum spin liquid in the spin-1/2 triangular antiferromagnet $\text{EtMe}_3\text{Sb}[\text{Pd}(\text{dmit})_2]_2$, *Phys. Rev. B* **77**, 104413 (2008).
- [12] M. Yamashita, N. Nakata, Y. Senshu, M. Nagata, H. M. Yamamoto, R. Kato, T. Shibauchi, and Y. Matsuda, Highly mobile gapless excitations in a two-dimensional candidate quantum spin liquid, *Science* **328**, 1246 (2010).
- [13] T. Itou, A. Oyamada, S. Maegawa, and R. Kato, Instability of a quantum spin liquid in an organic triangular-lattice antiferromagnet, *Nat. Phys.* **6**, 673 (2010).
- [14] T. Itou, K. Yamashita, M. Nishiyama, A. Oyamada, S. Maegawa, K. Kubo, and R. Kato, Nuclear magnetic resonance of the inequivalent carbon atoms in the organic spin-liquid material $\text{EtMe}_3\text{Sb}[\text{Pd}(\text{dmit})_2]_2$, *Phys. Rev. B* **84**, 094405 (2011).
- [15] S. Yamashita, T. Yamamoto, Y. Nakazawa, M. Tamura, and R. Kato, Gapless spin liquid of an organic triangular compound evidenced by thermodynamic measurements, *Nat. Commun.* **2**, 275 (2011).
- [16] D. Watanabe, M. Yamashita, S. Tonegawa, Y. Oshima, H. M. Yamamoto, R. Kato, I. Sheikin, K. Behnia, T. Terashima, S. Uji, T. Shibauchi, and Y. Matsuda, Novel Pauli-paramagnetic quantum phase in a Mott insulator, *Nat. Commun.* **3**, 1090 (2012).
- [17] Y. S. Li, H. Liao, Z. Zhang, S. Li, F. Jin, L. Ling, L. Zhang, Y. Zou, L. Pi, Z. Yang, J. Wang, Z. Wu, and Q. Zhang, Gapless quantum spin-liquid ground state in the two-dimensional spin-1/2 triangular antiferromagnet YbMgGaO_4 , *Sci. Rep.* **5**, 16419 (2015).
- [18] Y. Shen, Y. D. Li, H. Wo, Y. Li, S. Shen, B. Pan, Q. Wang, H. C. Walker, P. Steffens, M. Boehm, Y. Hao, D. L. Quintero-Castro, L. W. Harriger, M. D. Frontzek, L. Hao, S. Meng, Q. M. Zhang, G. Chen, and J. Zhao, Evidence for a spinon Fermi surface in a triangular lattice quantum-spin-liquid candidate, *Nature (London)* **540**, 559 (2016).
- [19] J. A. M. Paddison, M. Daum, Z. Dun, G. Ehlers, Y. Liu, M. B. Stone, H. Zhou, and M. Mourigal, Continuous

- excitations of the triangular-lattice quantum spin liquid YbMgGaO_4 , *Nat. Phys.* **13**, 117 (2017).
- [20] Y. Xu, J. Zhang, Y. S. Li, Y. J. Yu, X. C. Hong, Q. M. Zhang, and S. Y. Li, Absence of Magnetic Thermal Conductivity in the Quantum Spin-Liquid Candidate YbMgGaO_4 , *Phys. Rev. Lett.* **117**, 267202 (2016).
- [21] Z. Ma *et al.*, Spin-Glass Ground State in a Triangular-Lattice Compound YbZnGaO_4 , *Phys. Rev. Lett.* **120**, 087201 (2018).
- [22] Y. Li, D. Adroja, D. Voneshen, R. I. Bewley, Q. Zhang, A. A. Tsirlin, and P. Gegenwart, Nearest-neighbour resonating valence bonds in YbMgGaO_4 , *Nat. Commun.* **8**, 15814 (2017).
- [23] Y. Li, S. Bachus, B. Liu, I. Radelytskyi, A. Bertin, A. Schneidewind, Y. Tokiwa, A. A. Tsirlin, and P. Gegenwart, Rearrangement of Uncorrelated Valence Bonds Evidenced by Low-Energy Spin Excitations in YbMgGaO_4 , *Phys. Rev. Lett.* **122**, 137201 (2019).
- [24] R. Kato, Conducting metal dithiolene complexes: Structural and electronic properties, *Chem. Rev.* **104**, 5319 (2004).
- [25] K. Kanoda and R. Kato, Mott physics in organic conductors with triangular lattices, *Annu. Rev. Condens. Matter Phys.* **2**, 167 (2011).
- [26] M. Sutherland, D. G. Hawthorn, R. W. Hill, F. Ronning, S. Wakimoto, H. Zhang, C. Proust, E. Boaknin, C. Lupien, L. Taillefer, R. X. Liang, D. A. Bonn, W. N. Hardy, R. Gagnon, N. E. Hussey, T. Kimura, M. Nohara, and H. Takagi, Thermal conductivity across the phase diagram of cuprates: Low-energy quasiparticles and doping dependence of superconducting gap, *Phys. Rev. B* **67**, 174520 (2003).
- [27] S. Y. Li, J. B. Bonnemaïson, A. Payeur, P. Fournier, C. H. Wang, X. H. Chen, and L. Taillefer, Low-temperature phonon thermal conductivity of single crystalline Nd_2CuO_4 : Effects of sample size and surface roughness, *Phys. Rev. B* **77**, 134501 (2008).
- [28] B. J. Powell and R. H. McKenzie, Quantum frustration in organic Mott insulators: From spin liquids to unconventional superconductors, *Rep. Prog. Phys.* **74**, 056501 (2011).
- [29] C. P. Nave and P. A. Lee, Transport properties of a spinon Fermi surface coupled to a $U(1)$ gauge field, *Phys. Rev. B* **76**, 235124 (2007).
- [30] S. S. Lee and P. A. Lee, $U(1)$ Gauge Theory of the Hubbard Model: Spin Liquid States and Possible Application to κ -(BEDT-TTF) $_2\text{Cu}_2(\text{CN})_3$, *Phys. Rev. Lett.* **95**, 036403 (2005).
- [31] Y. Zhou and T.-K. Ng, Spin liquid states in the vicinity of a metal-insulator transition, *Phys. Rev. B* **88**, 165130 (2013).
- [32] Y. Werman, S. Chatterjee, S. C. Morampudi, and E. Berg, Signatures of Fractionalization in Spin Liquids from Interlayer Transport, *Phys. Rev. X* **8**, 031064 (2018).
- [33] M. Yamashita, T. Shibauchi, and Y. Matsuda, Thermal-transport studies on two-dimensional quantum spin liquids, *Chem. Phys. Chem.* **13**, 74 (2012).
- [34] K. Watanabe, H. Kawamura, H. Nakano, and Toru Sakai, Quantum spin-liquid behavior in the spin-1/2 random Heisenberg antiferromagnet on the triangular lattice, *J. Phys. Soc. Jpn.* **83**, 034714 (2014).
- [35] I. Kimchi, A. Nahum, and T. Senthil, Valence Bonds in Random Quantum Magnets: Theory and Application to YbMgGaO_4 , *Phys. Rev. X* **8**, 031028 (2018).
- [36] I. Kimchi, J. P. Sheckelton, T. M. McQueen, and P. A. Lee, Scaling and data collapse from local moments in frustrated disordered quantum spin systems, *Nat. Commun.* **9**, 4367 (2018).
- [37] P. Bourgeois-Hope, F. Laliberte, E. Lefrancois, G. Grissonnanche, S. R. de Cotret, R. Gordon, R. Kato, L. Taillefer, and N. Doiron-Leyraud, Thermal Conductivity of the Quantum Spin Liquid Candidate $\text{EtMe}_3\text{Sb}[\text{Pd}(\text{dmit})_2]_2$: No Evidence of Mobile Gapless Excitations, *Phys. Rev. X* **9**, 041051 (2019).